Cellular Physiology and Biochemistry

Cell Physiol Biochem 2012;30:791-804
DOI: 10.1159/000341458
Published online: August 07, 2012
Accepted: July 13, 2012

1015-8987/12/0303-0791$38.00/0

Original Paper

Murine GASP-1 *N*-Glycosylation is not Essential for its Activity on C2C12 Myogenic Cells but Alters its Secretion

Caroline Brun[a] Olivier Monestier[a] Sébastien Legardinier[a]
Abderrahman Maftah[a] Véronique Blanquet[a]

[a]INRA, UMR1061 Génétique Moléculaire Animale - Université de Limoges, FR 3503 GEIST, Faculté des Sciences et Techniques, 87060 Limoges, France

Key Words
GASP-1 • GDF8 • Glycosylation • Secretion • Myogenesis

Abstract
Background/Aims: Growth and differentiation factor-associated serum protein-1 (GASP-1) is a secreted protein known to be capable of binding and inhibiting the activity of several TGF-beta family members, including myostatin. The present study was designed to characterize murine GASP-1 post-translational modifications and to determine their influence on the biological activity of GASP-1. ***Methods:*** We describe herein the site-directed mutagenesis of single *N*-glycosylation sites and combinations of them in 4 mutants of murine GASP-1. ***Results:*** *In vitro* and *in vivo* analysis revealed that GASP-1 is a glycoprotein containing 2 *N*-glycans and several mucin-type *O*-glycans. Treatments by the recombinant murine GASP-1 protein enhance C2C12 proliferation and differentiation by inhibition of the myostatin pathway. The loss of *N*-glycans leads to a decrease in protein secretion rate but does not affect its ability to activate myogenesis. ***Conclusion:*** Analysis of structure-function relationships of murine GASP-1 provides insights into the involvement of the carbohydrate moiety of mGASP-1 on its biological activity.

Véronique Blanquet

Institut National de Recherche Agronomique, UMR 1061, Génétique Moléculaire Animale, FR 3503 GEIST, Faculté des Sciences et Techniques,123, avenue Albert Thomas, 87060 Limoges Cedex (France) Tel. +33 555457664, E-Mail veronique.blanquet@unilim.fr

Introduction

Skeletal muscle development and growth are tightly regulated processes involving multiple factors that control different cellular programs such as proliferation, differentiation and fusion [1-6]. Myostatin (GDF8), a member of TGF-beta family, is a protein mostly secreted by skeletal muscle and acts as a potent negative regulator of myogenic proliferation and differentiation as well as muscle stem cell activation and self-renewal [7, 8]. Loss of a functional GDF8 protein or overexpression of its inhibitors lead to a significant increase of muscle mass [9-11]. Among the myostatin-binding proteins, GASP-1 has been identified in mouse and human sera [12]. GASP-1 was shown to bind *in vitro* directly and independently both mature myostatin and its propeptide but also other TGF-beta such as TGFβ1, BMP2, BMP4. However, GASP-1 inhibits only myostatin activity [12, 13]. It might also block myostatin proprotein processing through inhibition of furin-like protease as Hill et al. reported [12]. GASP-1 is a secreted protein that contains multiple domains associated with protease-inhibitory proteins including a whey acidic protein (WAP) domain, a kazal domain, two kunitz domains, and a netrin domain. It also contains a highly conserved module of cysteine-rich sequence termed the follistatin domain. The WAP and follistatin/kazal modules are assumed to be responsible for the interaction with TGF-beta whereas the netrin domain would be involved in the interaction with the propeptide [14]. This domain organization suggests that GASP-1 may serve to control the action of diverse serine proteases as well as metalloproteinases. To further understand the *in vivo* roles of GASP-1, we generated a gain-of-function transgenic mouse model that overexpresses *Gasp-1* under transcriptional control of the human cytomegalovirus immediate-early promoter/enhancer (unpublished data). GASP-1 expression analysis in different tissues of these transgenic mice revealed that the secreted GASP-1 has an apparent molecular mass of 70-80 kDa, higher than the predicted one [14]. Indeed, the primary structure of mouse GASP-1 corresponds to a 571 amino acids protein comprising the signal peptide, with a molecular weight of 63.33 kDa. Since the analysis was done under reducing conditions, the structural difference between the two forms is more likely due to post-translational modifications of GASP-1 than protein complex isoform and subcomplex compositions.

Glycosylation has been studied intensively for the past two decades as the most common covalent protein modification in eukaryotic cells, with significant effects on protein folding, conformation, distribution, stability and activity [15]. A glycoprotein might be *N*-glycosylated (oligosaccharides are added to asparagine found in a Asn-X-Ser/Thr consensus sequence), *O*-glycosylated (glycans are linked to Ser/Thr residues) or both. Therefore, glycoprotein properties are strongly influenced by the overall size, shape and charge of the glycan [16].

In the present study, we address the question of whether GASP-1 undergoes *N*- and/or *O*-linked glycosylation and investigate the importance of different glycoforms in GASP-1 biological activities, particularly its inhibitor function on myostatin's actions. Thus, we produced the recombinant murine GASP-1 protein in eukaryotic cells and characterized its post-translational modifications. Using site-directed mutagenesis, we demonstrate that (i) *N*-glycosylation is not a prerequisite for GASP-1 secretion, (ii) deletion of all *N*-glycosylation sites significantly reduced its secretion efficiency but not its ability to activate myogenesis.

Materials and Methods

Cell lines and cell staining

C2C12 mouse myoblast cells (ATCC - CRL-1772) and COS-7 monkey kidney cells (ATCC - CRL-1651) were maintained at 37°C in Dulbecco's modified Eagle's medium (DMEM), supplemented with 10% heat-inactivated fetal bovine serum (FBS), 100 units.ml^{-1} penicillin and 100 µg.ml^{-1} streptomycin (Growth Medium, GM). To induce C2C12 differentiation, cells at 70% confluence were shifted to DMEM containing 2% horse serum (Differentiating Medium, DM). The medium was changed every day. Cells were washed two times in phosphate-buffered saline (PBS) before fixing in paraformaldehyde 4%/PBS 1X for 15 min.

Next, cells were rinsed two times in PBS and dehydrated in 70% ethanol overnight. Cells were then stained with hematoxylin (Thermo Scientific) for 20 min, washed in PBS, stained with eosin (Thermo Scientific) for 10 min and finally washed in PBS. Fusion index of C2C12 cells was calculated as the ratio of the number of nuclei in multinucleated cells to the total number of nuclei in 12 different fields/well.

SurGasp1-20 tissues

SurGasp1-20 is a transgenic mouse line that ubiquitously overexpresses *Gasp-1* under the control of a cytomegalovirus promoter (unpublished data). Total proteins were extracted from different tissues among which skeletal muscles dissected from 12-week-old surGasp1-20 mice using lysis buffer (50 mM Tris, pH 8, 150 mM NaCl, 0.1% SDS, 1% NP-40, 0.5% sodium deoxycholate, and protease inhibitors). Plasma was diluted 20 times in lysis buffer.

Bioinformatics analysis

GASP-1 orthologs were retrieved from databases using BLAST (http://www.ncbi.nlm.nih.gov/BLAST) and Ensembl Genome Browser (www.ensembl.org). Alignment was performed using ClustalW program and analyzed with WebLogo. Asparagine and serine/threonine residues potentially glycosylated were identified using respectively NetNGlyc 1.0 Server (http://www.cbs.dtu.dk/services/NetNGlyc/) and NetOGlyc 3.1 Server [17].

Subcloning and site-directed mutagenesis of mGASP-1

The mouse *Gasp-1* cDNA coding sequence was amplified from mouse cDNA using specific primers (sense, 5'-ATGTGTGCCCCAGGGTATCATCG-3'; antisense, 5'-TTGCAAGCCCAGGAAGTCCTTGAG-3') under the following conditions: 94°C for 30 s, 60°C for 30 s, 72°C for 2 min followed by 35 cycles. The amplified cDNA was cloned into the TOPO sites of the pcDNA3.1/V5-His-TOPO vector (Invitrogen) in order to include an in-frame C-terminal V5-polyhistidine (His) tag, thus generating the pGasp-1 expression vector. The N178Q, N314Q and N514Q mutant constructs were generated from the pGasp-1 vector using the GENEART Site-Directed Mutagenesis System (Invitrogen). The reaction was carried out with 20 ng of vector, 0.3 µM of sense and reverse primers (for N178Q, sense 5'-CGTTATCACTTCACCTGGCCT**CAA**ACCAGCCCTCCACCGCC-3' and reverse 5'-GGCGGTGGAGGGCTGGT**TTG**AGGCCAGGTGAAGTGATAACG-3', for N314Q, sense 5'-GCCACTTCAGAGAGCAGTCTC**CAA**GGCACAGCTTTTCCAGC-3' and reverse 5'-GCTGGAAAAGCTGTGCC**TTG**GAGACTGCTCTCTGAAGTGGC-3', for N514Q, sense 5'-CTGGACCTGTCCTTGCCCC**CAA**GTGACAGTGGGTGAGACAC-3' and reverse 5'-GTGTCTCACCCACTGTCAC**TTG**GGGGCAAGGACAGGTCCAG-3') and 1U of AccuPrime *Pfx* DNA Polymerase (Invitrogen). The double (N178/314Q, N178/514Q, N314/514Q) or triple mutants (N178/314/514Q) were produced from the single or double mutants as template. The sequence-verified plasmids were used to transiently transfect COS-7 and CHO-K1 cells.

Transient transfections of COS-7 cells

COS-7 cells at 70% confluence were transiently transfected using the XtremeGENE 9 Transfection Reagent (Roche Applied Science) with 5 µg of each construct in DMEM serum-free media. 72h after transfection, 20 µl of supernatants from each culture were tested in Western blot, and 20 ml media were recovered by centrifugation for the nickel affinity purification.

Nickel affinity purification of wild-type and mutated murine GASP-1 produced in COS-7 cells

20 ml supernatants were concentrated by centrifugation at 3000g with 30K Amicon Ultra-4 Centrifugal Filter Units (Millipore) exchanged with a binding buffer (50 mM NaH_2PO_4, pH 8, 300 mM NaCl, 20 mM Imidazole) and incubated with 50 µl Ni-NTA magnetic beads (Qiagen Inc) at 4°C overnight. After incubation, nonspecific proteins were removed from beads with a washing buffer (50 mM NaH_2PO_4, pH 8, 300 mM NaCl, 20 mM Imidazole, 0.005% Tween-20). Bound proteins were eluted in 50µl of elution buffer (50 mM NaH_2PO_4, pH 8, 300 mM NaCl, 250 mM Imidazole, 0.005% Tween-20).

SDS-PAGE and western blot analysis

Total proteins (50 µg) from SurGasp1-20 tissues and total proteins from C2C12 treated with 500 $ng.ml^{-1}$ mGASP-1 and/or 250 $ng.ml^{-1}$ human GDF8 (788-G8, R&D Systems) were quantified at A_{595nm} using the Bradford assay. 10 µl of 20-times diluted plasma were analyzed. These proteins and

250 ng of purified mGASP-1 proteins were mixed with Laemmli loading buffer and heated for 5 min at 95°C. The proteins were separated under denaturating and reducing conditions into a 10% polyacrylamide gel and then transferred onto a Hybond C-Extra Nitrocellulose membrane (GE Healthcare). Unspecific binding was prevented using 5% non fat dry milk (w/v) in TBST0.1% buffer (50 mM Tris-HCl, 150 mM NaCl, pH 7.4, 0.1% Tween-20) for 1h at room temperature. Incubation with the primary antibodies [Polyclonal Goat anti-hGASP-1 antibody (AF2070, R&D Systems, 0.2 $\mu g.ml^{-1}$); Polyclonal Rabbit anti-hGASP-1 (HPA010953, Sigma, 0.3$\mu g.ml^{-1}$); Rabbit anti-mGASP-1 directed against the peptide, (DCGEEQTRWFDAQANN, 0.9 $\mu g.ml^{-1}$); Polyclonal Goat anti-mouse Smad2/3 antibody, (AF3797, 0.5 $\mu g.ml^{-1}$); Polyclonal Rabbit anti-human phospho-Smad3 antibody, (AB3226, 0.4 $\mu g.ml^{-1}$); Polyclonal Goat anti-mouse GAPDH antibody, (AF5718, 0.2 $\mu g.ml^{-1}$)] diluted in 2% non fat dry milk in TBST0.1% buffer took place overnight at 4°C, followed by several washing steps in TBST0.1%. Blots were incubated with horseradish peroxidase-coupled anti-goat IgG or anti-rabbit IgG (Dako) at a dilution of 1:1000 in 2% non fat dry milk in TBST0.1% buffer for 1h at RT. After several washing steps in TBST0.1%, immunoblots were developed by enhanced chemiluminescence using by BM Chemiluminescence Western Blotting Substrate (POD) (Roche Applied Science) and exposed to a film (GE Healthcare Hyperfilm ECL, GE Healthcare).

Glycosylation analysis

N-deglycosylation. 250 ng of purified proteins or 50 µg of total proteins from mice tissues were denatured at 95°C for 10 min in 10 mM potassium phosphate and 0.2% SDS. The samples were then incubated overnight at 37°C in a buffer (10mM potassium phosphate, pH8, 10 mM EDTA, 0.5% Triton X-100, 0.2% SDS, 1% β-mercaptoethanol) containing 0.1-1U of PNGase F (Roche Applied Science).

O-deglycosylation. The *O*-deglycosylation was performed with the EDEGLY kit (Sigma-Aldrich). 250 ng of purified proteins or 50 µg of total proteins from mice tissues were denatured at 100°C for 5 min in 2.5 µl of denaturation solution (Sigma-Aldrich) and 10 µl of reaction buffer 5X. Samples were incubated overnight at 37°C with 1µl of each enzyme (PNGase F, *O*-Glycosidase, α-(2→3,6,8,9)-Neuraminidase, β-N-Acetylglucosaminidase, β-(1→4)-Galactosidase).

Lectin blot analysis. The DIG Glycan Differentiation kit (Roche Applied Science) was used. GASP-1 and control glycoproteins (Fetuin and Carboxypeptidase Y) treated or not with PNGase F were separated on a 10% polyacrylamide gel under denaturating conditions and transferred on a nitrocellulose membrane. After saturation for 2h at room temperature (RT) with blocking reagent, membranes were washed in TBST0.05%, and they were incubated overnight at RT with each digoxigenin labeled lectin (1$\mu g.ml^{-1}$ MAA, 0.2 $\mu g.ml^{-1}$ SNA) in TBST0.05% complemented by 1mM $CaCl_2$, 1mM $MgCl_2$, 1mM $MnCl_2$. After several washing steps, membranes were incubated with the anti-digoxigenin-AP at a dilution of 1:1000 in TBST0.05% for 1h at RT and revealed with a NBT/BCIP solution.

Quantitation of expressed recombinant GASP-1

Concentrations of recombinant GASP-1 proteins produced in COS-7 cells culture media were determined in a sandwich ELISA (GASP-1 DuoSet ELISA kit, R&D Systems), as described previously [18]. All measurements were performed in triplicate and data for the standard curve were fitted to a logistic plot to calculate the levels of mGASP-1.

Myoblast proliferation assay

C2C12 myoblasts were seeded at 2.000 cells per well in Growth Medium in 96-well microtiter plates. After 24h, cells were treated with recombinant mGASP-1 (0 to 2 $\mu g.ml^{-1}$) or *N*-glycosylation mutant (1 $\mu g.ml^{-1}$) proteins. Plates were incubated at 37°C in atmosphere of 5% CO_2 for a further 48h, prior to the addition of 20µL of MTS solution (CellTiter 96® AQ_{ueous} Non-Radioactive Cell Proliferation Assay, Promega). Absorbance at 490nm of the formazan product from bioreduced MTS was read using an ELISA plate reader.

Time course of C2C12 differentiation

Myoblast cells were grown to 80% confluence and were differentiated into myotubes after shifting GM in DM supplemented or not by 1 $\mu g.ml^{-1}$ mGASP-1 for 96 h. For each kinetic point analysed, cells were washed briefly with 1X PBS and harvested following trypsinization.

RNA extraction, cDNA synthesis and gene expression analysis

Total RNA from each kinetic point was obtained by anion exchange chromatography (RNeasy mini Kit, Qiagen Inc). The High Capacity cDNA reverse transcription Kit (Applied Biosystems) was used to convert 4 µg of total RNA into single-stranded cDNA. Taqman primers and probe sets for two target genes (myogenin and p21) and two endogenous control genes (Dffa, beta-2 microglobulin) were used. Quantitative PCR reaction was performed from 50 ng of cDNA in a ABI Prism 7900HT Sequence Detection System (Applied Biosystems) using 40 cycles of 95°C for 15 sec followed by 60°C for 1 min.

Statistical analysis

Unless indicated otherwise, data are presented as mean ± SD. Data are considered significant with P value < 0.05 by ANOVA test analysis.

Results

Expression of recombinant Histidine-tagged mGASP-1 protein

To study post-translational modifications of GASP-1, we produced the mouse protein as a C-terminal V5/His-tagged fusion protein in COS-7 cells transiently transfected with the pGasp-1 vector. The purified secreted protein was revealed as a major protein of 76 kDa either by Coomassie blue staining or by three specific anti-GASP-1 antibodies (Fig. 1). The protein identity was confirmed by nanoflow-LC-MS/MS (Table 1).

In silico analysis of potential glycosylation sites of murine GASP-1

Murine GASP-1 is a 571 amino acid protein. Like its human counterpart, it contains a signal sequence, a WAP domain, a follistatin/kazal domain, an Igc2 domain, two BPTI/kunitz domains and a netrin domain (Fig. 2A). *In silico* analysis of GASP-1 with the NetNGlyc Server revealed three consensus *N*-glycosylation sites at asparagine N178, N314, and N514 (Fig. 2B). According to the graph, the N178 was less likely to be glycosylated as the signal was below the threshold. The NetOGlyc Server allowed us to highlight 9 serine or threonine, T175, T179, S180, T186, T187, T191, T192, S194 and T197 (Fig. 2C) with a mucin-type *O*-glycosylation potential higher than the threshold. All of them were located between the follistatin/kazal and the Igc2 domains.

To examine different glycosylation sites conservation, we performed an alignment of GASP-1 primary sequences of 30 vertebrates and each sequence of interest was then represented with Weblogo (Fig. 2D and 2E). The sequence logos indicated that the first potential *N*-glycosylation site, N178, was less conserved than the two others, N314 and N514. This result was correlated with that predicted by NetNGlyc (Fig. 2D). In addition, at the exception of S194, all the potential *O*-glycosylation sites were conserved among vertebrates (Fig. 2E).

In vitro and in vivo evaluations of mGASP-1 states of glycosylation

As the recombinant mGASP-1 protein secreted either from COS-7 or surGasp1-20 mice plasma displayed identical electrophoretic mobilities (Fig. 3), their glycosylation status is undoubtedly close, allowing us to perform all analysis on the purified recombinant protein. We first investigated mGASP-1 glycosylation states by enzymatic digestions. Western analysis after *N*-deglycosylation by PNGase F or *O*-deglycosylation by four other enzymes (*O*-Glycosidase, α-(2→3,6,8,9)-Neuraminidase, β-N-Acetylglucosaminidase, β-(1→4)-Galactosidase) revealed that mGASP-1 migrated faster than the untreated protein, at 71 and 70 kDa respectively (Fig. 3A). Finally, poly-histidine-tagged mGASP-1 fully deglycosylated migrated at 65 kDa (Fig. 3A, lane 4) like the expected molecular weight, suggesting that mGASP-1 is *N*- and *O*-glycosylated.

We intended to further characterize mGASP-1 glycosylation in various mouse tissues. Unfortunately, we were not able to detect the endogenous GASP-1 protein by western blotting in protein samples from wild type mice. This might be explained by low expression

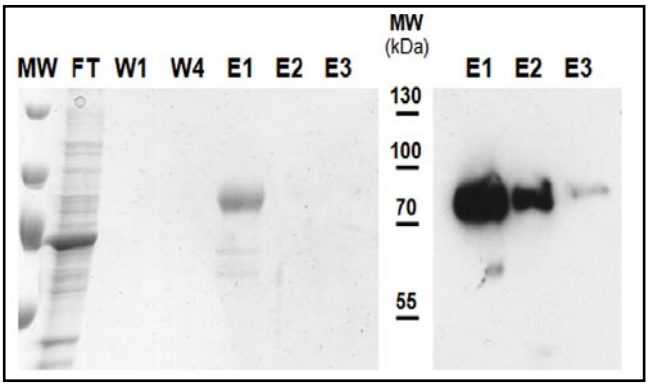

Fig. 1. Purified recombinant mGASP-1. (left blot) After COS-7 medium concentration and purification by Ni-NTA magnetic agarose beads, eluted mGASP-1 was revealed in the first eluate (E1) by Coomassie Blue-staining of SDS-PAGE. (right blot) Western blot analysis revealed the purified mGASP-1 protein in the three successive eluates (E1-3) by specific anti-GASP-1 antibodies. MW, molecular weight marker; FT, flow-through; W, washes; E, eluate.

Table 1. GASP-1 peptides identified in first Ni-NTA purification eluate by LC-MS/MS.

Peptide sequences	m/z	z	M exp	Score	E value
(K)LVTSFC*R(S)	441,6211	2	881,2276	50	0,00048
(R)ADFPLSVVR(G)	502,1535	2	1002,2924	46	0,0013
(R)ALVTVDEVLK(D)	543,7056	2	1085,3966	42	0,0031
(K)GITLSVVTC*R(Y)	553,1833	2	1104,3521	42	0,0036
(R)VSELTEEQDSGR(A)	675,1635	2	1348,3125	83	2,10E-07
(R)EAC*EESC*PFPR(G)	691,236	2	1380,4575	84	1,80E-07
(R)ALVTVDEVLKDEK(M)	729,742	2	1457,4695	74	2,00E-06
(R)EC*ETDQEC*ETYEK(C)	860,7456	2	1719,4767	73	2,10E-06
(K)EPSFTC*ASDGLTYYNR(C)	940,7431	2	1879,4717	82	2,40E-07
(R)YSHAGIC*PNDMNPNLWVDAQSTC*K (R)	931,9715	3	2792,8927	60	2,40E-05

C* : Carbamidomethyl (C)

level of GASP-1. Therefore, we decided to perform our study from tissues of transgenic mice overexpressing ubiquitously *Gasp-1*. Using three different specific antibodies, it appeared that in all samples, GASP-1 presented a very specific four bands migration profile compared to that of the plasma protein (Fig. 3B). After PNGase F treatment, only two bands remained present and the lowest one migrated at the predicted mass without any post-translational modifications. After removing the mucin-type *O*-glycans, we observed two bands corresponding to the two lowest bands of the untreated tissue. The removal of both *N*- and *O*-glycans led to a protein of ~60 kDa similar to the predicted mass of tissue mGASP-1 (60.7 kDa) (Fig. 3B). Taken together, these data indicate that mGASP-1 could be found as a form without mucin-type *O*-glycans (black arrows) and a form with both *N*- and *O*-glycans (grey arrows). In addition, mGASP-1 could be mono-*N*-glycosylated (solid arrows) or di-*N*-glycosylated (dashed arrows). The same observations were found in all other tissues (data not shown).

Site-specific N-glycosylation analysis of mGASP-1

To determine whether each *N*-glycosylation site was occupied, the three asparagine were separately converted into glutamine by site-directed mutagenesis. In parallel of pGasp-1, each *N*-glycosylation mutant vector, N178Q, N314Q, and N514Q, was transiently transfected into COS-7 cells. The recombinant proteins were produced for 3 days in a serum-free media, purified, and then resolved on SDS-PAGE. Western blot analysis showed that the N178Q protein migrated at the same position than the wild-type mGASP-1 indicating that N178 site was not glycosylated in the wild-type protein (Fig. 4). On the contrary, the mutant N314Q or N514Q proteins migrated faster than mGASP-1 (Fig. 4). These results indicated that the two sites were glycosylated in the wild-type mGASP-1 and were confirmed by a PNGase F digestion showing an identical profile migration at 71 kDa of each *N*-deglycosylated mutant (Fig. 4). The same experiments were conducted on each double

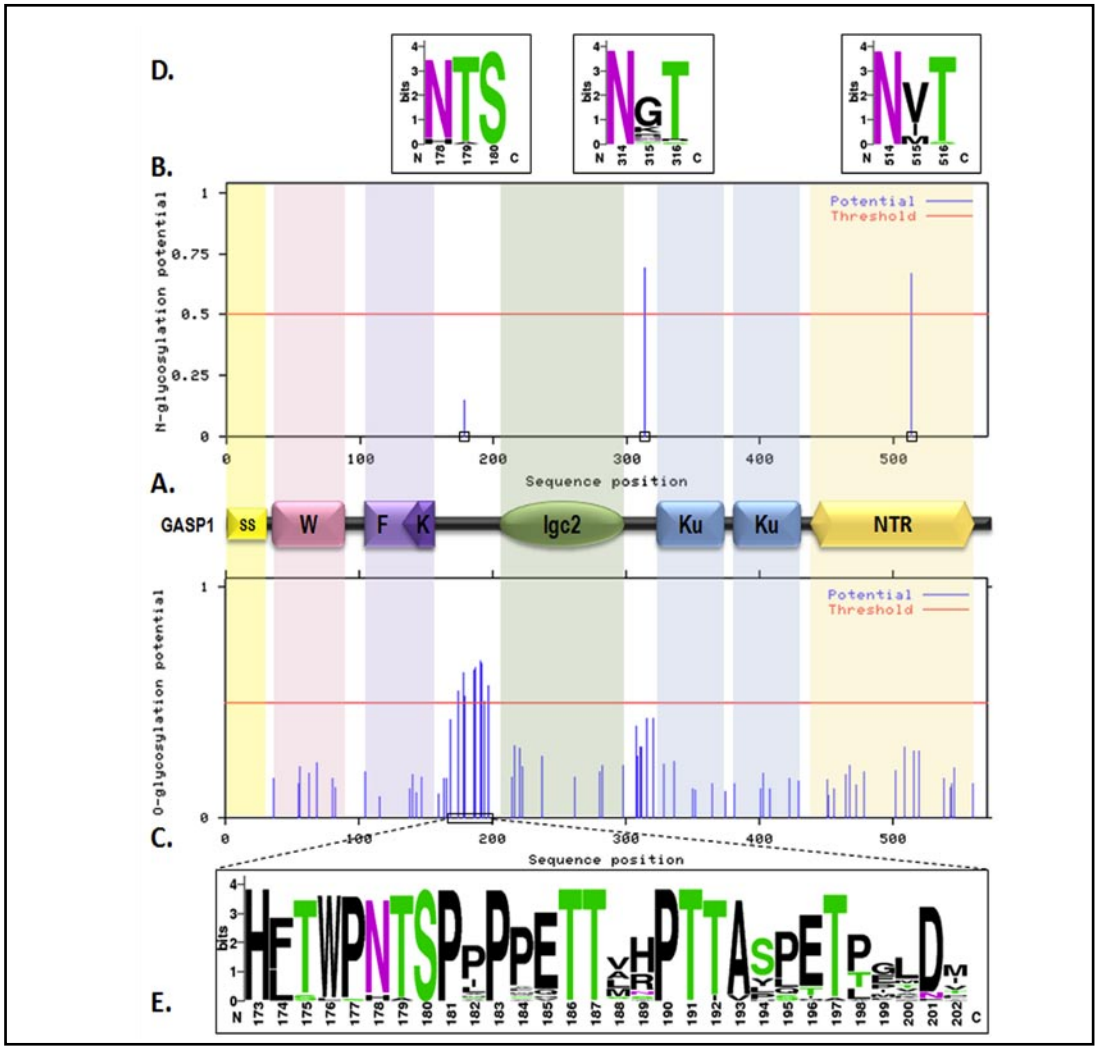

Fig. 2. Identification and conservation among vertebrates of *N*- and *O*-glycosylation sites. (A) Structure of mGASP-1. mGASP-1 has a signal sequence (SS), a WAP domain (W), a follistatin domain (F), an Igc2 domain, two BPTI/kunitz domains (Ku), a netrin domain (NTR). (B) mGASP-1 has three *N*-glycosylation consensus sequences at aspargyl residues 178, 314 and 514, with two potential sites (N314 and N514). (C) mGASP-1 has nine potential mucin-type *O*-glycosylation sites (T175, T179, S180, T186, T187, T191, T192, S194 and T197). (D, E) WebLogos are formed through the comparison of 30 sequences of vertebrates and illustrated the conservation of each potential glycosylation site (the taller the logo, the lesser is the variability at the site).

mutant and the triple mutant. N178/314Q and N178/514Q double mutants had the same molecular weight and migrated faster after PNGase F treatment. The N314/514Q double mutant and N178/314/514Q triple mutant migrated at 71 kDa, with or without *N*-deglycosylation (Fig. 4), confirming that mGASP-1 had only two *N*-glycans on N314 and N514. We found similar results when using CHO-K1 cells as another line to produce GASP-1 recombinant proteins (data not shown).

To further analyze glycan structures of mGASP-1, *Maackia amurensis* agglutinin (MAA) and *Sambucus nigra* agglutinin (SNA) were used to distinguish the type of sialic acid (Sia) linkage on *N*- and/or *O*-linked carbohydrate side chains (Fig. 5). MAA recognizes specifically Sia linked as α-(2→3) galactose on *N*- and/or *O*-linked glycans while SNA recognizes specifically Sia linked as α-(2→6) galactose on carbohydrate side chains. As seen on figure

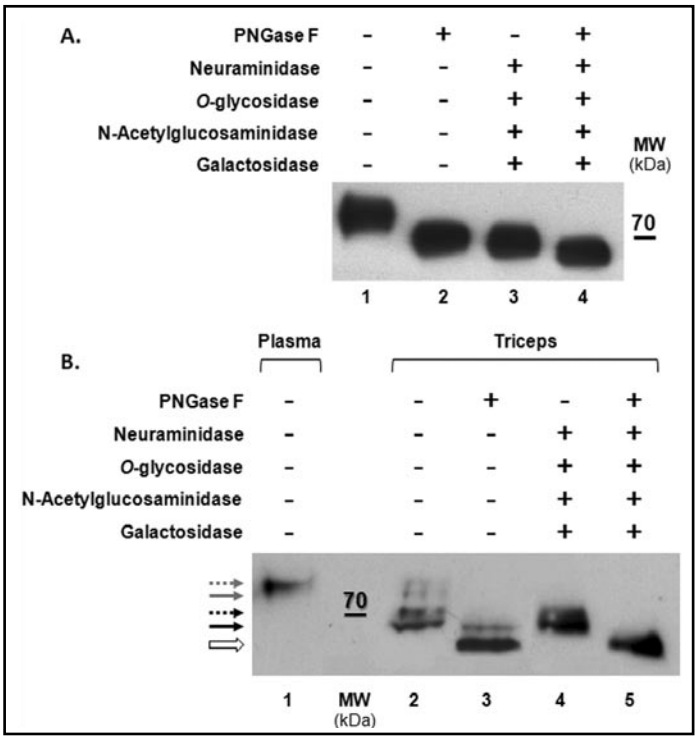

Fig. 3. Western blot analysis of mGASP-1 produced in COS-7 or from SurGasp1-20 mice tissues sequentially deglycosylated. (A) Glycosylated (lane 1), *N*-deglycosylated (lane 2), *O*-deglycosylated (lane 3), and fully deglycosylated GASP-1 (lane 4) purified from COS-7 supernatants were resolved by 10% SDS-PAGE and electroblotted onto nitrocellulose. Immunoblotting was conducted with specific anti-GASP-1 antibodies. (B) Total proteins extracted from triceps and plasma were treated with and without glycosidases. Plasma proteins (lane 1) and triceps proteins (glycosylated, lane 2; *N*-deglycosylated, lane 3; *O*-deglycosylated, lane 4; and fully deglycosylated, lane 5) were resolved by SDS-PAGE and immunoblotted with specific anti-GASP-1 antibodies. Solid black arrow, mono-*N*-glycosylated GASP-1; dashed black arrow, di-*N*-glycosylated GASP-1; solid grey arrow, mono-*N*-glycosylated and *O*-glycosylated GASP-1; dashed grey arrow, di-*N*-glycosylated and *O*-glycosylated GASP-1; solid white arrow, deglycosylated GASP-1. MW, molecular weight marker.

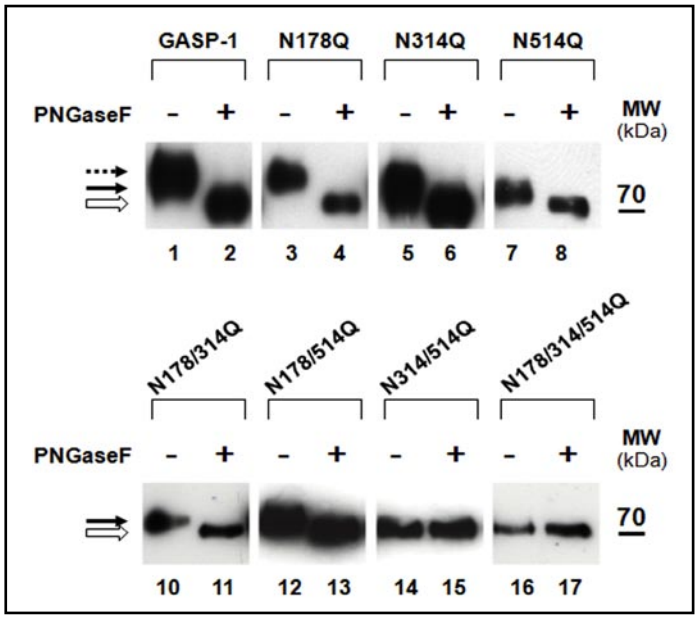

Fig. 4. mGASP-1 *N*-glycosylation sites occupancy. Purified mGASP-1 and its mutants were incubated with or without PNGase F and then, resolved by SDS-PAGE and immunoblotted using an antibody specific to GASP-1. Dashed black arrow, di-*N*-glycosylated GASP-1; solid black arrow, mono-*N*-glycosylated GASP-1; solid white arrow, *N*-deglycosylated GASP-1. MW, molecular weight marker.

5B, MAA bound to glycosylated and *N*-deglycosylated mGASP-1 protein but no signal was detected for the deglycosylated protein. With the SNA lectin, the only signal was seen on the complete glycosylated protein (Fig. 5C).

Surprisingly, all the mutants were secreted from COS-7 cells, even those entirely *N*-deglycosylated. Thus, we determined whether removing *N*-glycans at different sites alters GASP-1 secretion level. The N178Q, N178/314Q, N178/514Q and the triple

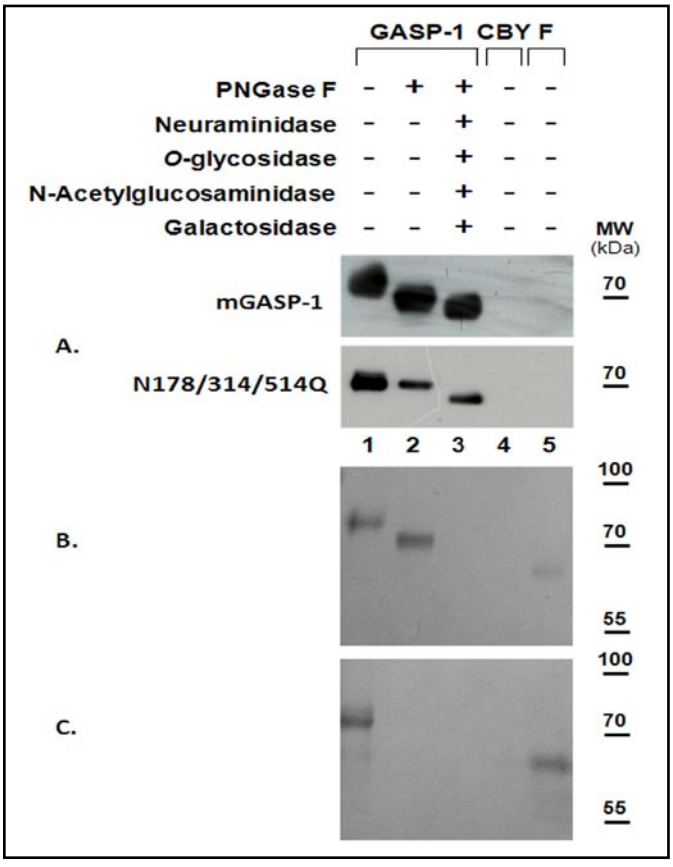

Fig. 5. Lectin blot analysis of mGASP-1. (A) mGASP-1 and triple mutant N178/314/514Q were resolved on SDS-PAGE without treatment (lane 1), or after *N*-deglycosylation (lane 2), or after complete deglycosylation (lane 3), and revealed with an anti-GASP-1 antibody. Carboxypeptidase Y (CBY), which is not sialylated, was used as a negative control of SNA and MAA (lane 4), and fetuin (F), which has Siaα2,3Gal and Siaα2,6Gal, as a positive control (lane 5). (B) 250 ng of purified mGASP-1 proteins were revealed by MAA (Maakia amurensis agglutinin) lectin which recognizes specifically Sia linked as α-(2→3) galactose. (C) 250 ng of purified mGASP-1 proteins were revealed by SNA (Sambucus nigra agglutinin) lectin which recognizes specifically Sia linked as α-(2→6) galactose. MW, molecular weight marker.

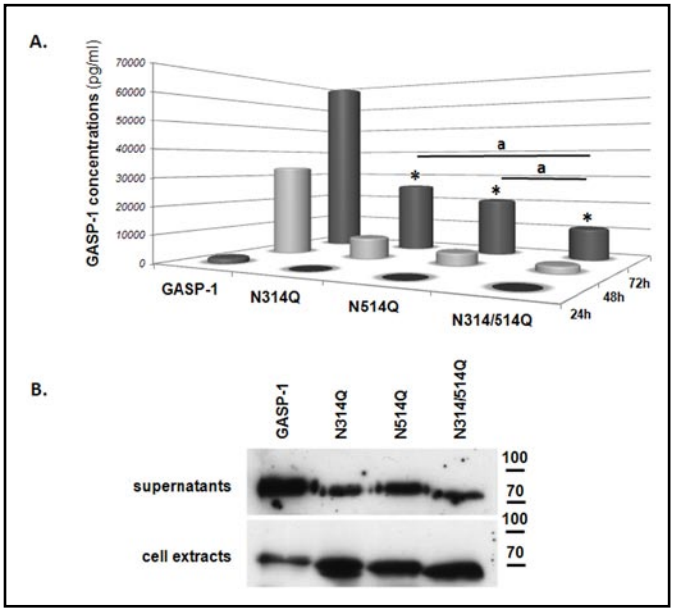

Fig. 6. Effects of loss of *N*-glycans on GASP-1 secretion. COS-7 cells were transiently transfected with the different *Gasp-1* plasmids. (A) Each day during 3 days, concentrations of recombinant GASP-1 proteins produced in culture media were determined in a sandwich ELISA. Statistical significance for mGASP-1 versus its *N*-glycosylation mutants and for N314/514Q versus N314Q or N514Q, represented by * and a respectively, was determined using ANOVA analysis. A P value < 0.05 was considered significant. (B) 15 µl of transfected COS-7 supernatants or 50 µg of total proteins extracted from transfected COS-7 were resolved by SDS-PAGE and immunoblotted with specific anti-GASP-1 antibodies.

mutants were excluded as N178 is not glycosylated. The loss of *N*-glycans led to a decrease of mGASP-1 secretion (Fig. 6A) and was confirmed by Western blot on supernatants and cells extracts (Fig. 6B). Each *N*-glycan seemed to be important for secretion as the double mutant N314/514Q was significantly less produced than the two simple mutants N314Q and N514Q (Fig. 6).

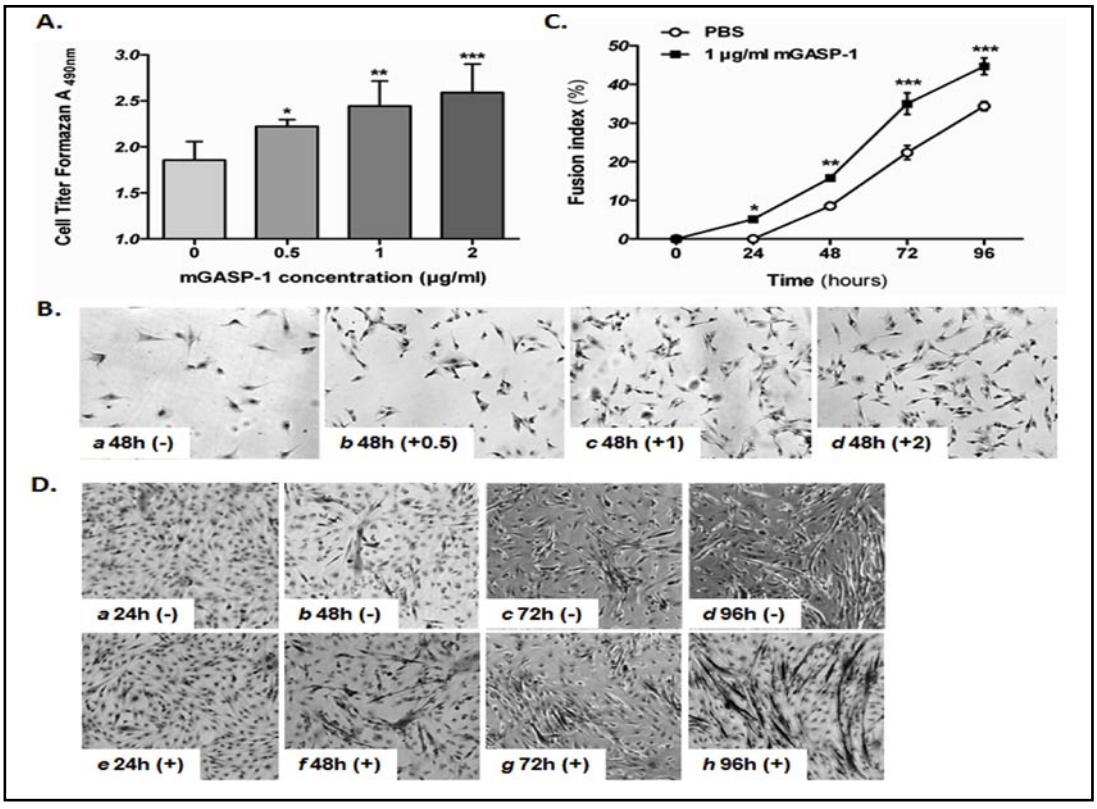

Fig. 7. mGASP-1 enhances C2C12 myoblast proliferation and differentiation. (A) C2C12 myoblasts were plated at 2000 cells/well for 1 day and then grown for 48h in the presence of increasing concentrations of mGASP-1 (0-2 µg.ml^{-1}), followed by Formazan assay. Each histogram corresponds to the mean ± S.D. of three independent experiments. (B) Cells were cultured without mGASP-1 (a) or with 0.5, 1 or 2 µg.ml^{-1} mGASP-1 (b, c, d) during 2 days and then, cells were fixed and stained with hematoxylin and eosin (x 400). (C) C2C12 myoblasts were cultured without mGASP-1 or in the presence of 1 µg.ml^{-1} mGASP-1, and fusion index were defined. Each point corresponds to the mean ± S.D. of three experiments. (D) Cells were fixed and stained with hematoxylin and eosin (x 100). Statistical significance for mGASP-1 concentrations of 0.5 to 2 µg.ml^{-1} versus none was determined using a ANOVA analysis. A *P* value < 0.05 was considered significant. * : *P* value < 0.05; ** : *P* value < 0.01; *** : *P* value < 0.005.

Effect of mGASP-1 and its N-deglycosylated forms on proliferation and differentiation of C2C12 myoblast cells

When GASP-1 was identified, it was shown that it binds to GDF8 and acts as an inhibitor of TGFβ signaling pathway [12]. Considering this function, we hypothesized that mGASP-1 might act as a regulator of myogenic proliferation and differentiation. To test this hypothesis, we treated C2C12 myoblast cells with various concentrations of the recombinant mGASP-1 protein (Fig. 7). Cell proliferation assay and cell staining showed that mGASP-1 treatment improved C2C12 myoblast proliferation in a dose-dependent manner (Fig. 7A and 7B). In addition, to test mGASP-1 ability to regulate C2C12 differentiation, cells were treated with 1 µg.ml^{-1} mGASP-1 for 96 h. We showed that mGASP-1 enhanced C2C12 differentiation as we observed fused cells at 24h of treatment whereas no fusion was observed in untreated cells. This difference was apparent over the time course (Fig. 7C and 7D). To determine if the increase of C2C12 myogenesis induced by the addition of mGASP-1 was due to a decrease of the GDF8 activity, phospho-Smad3 rates of C2C12 treated by GDF8 and/or GASP-1 were analyzed by Western blotting (Fig. 8A). As expected, addition of GDF8 on C2C12 cells led to an increase of the pSmad3 rate compared to the untreated control cells.

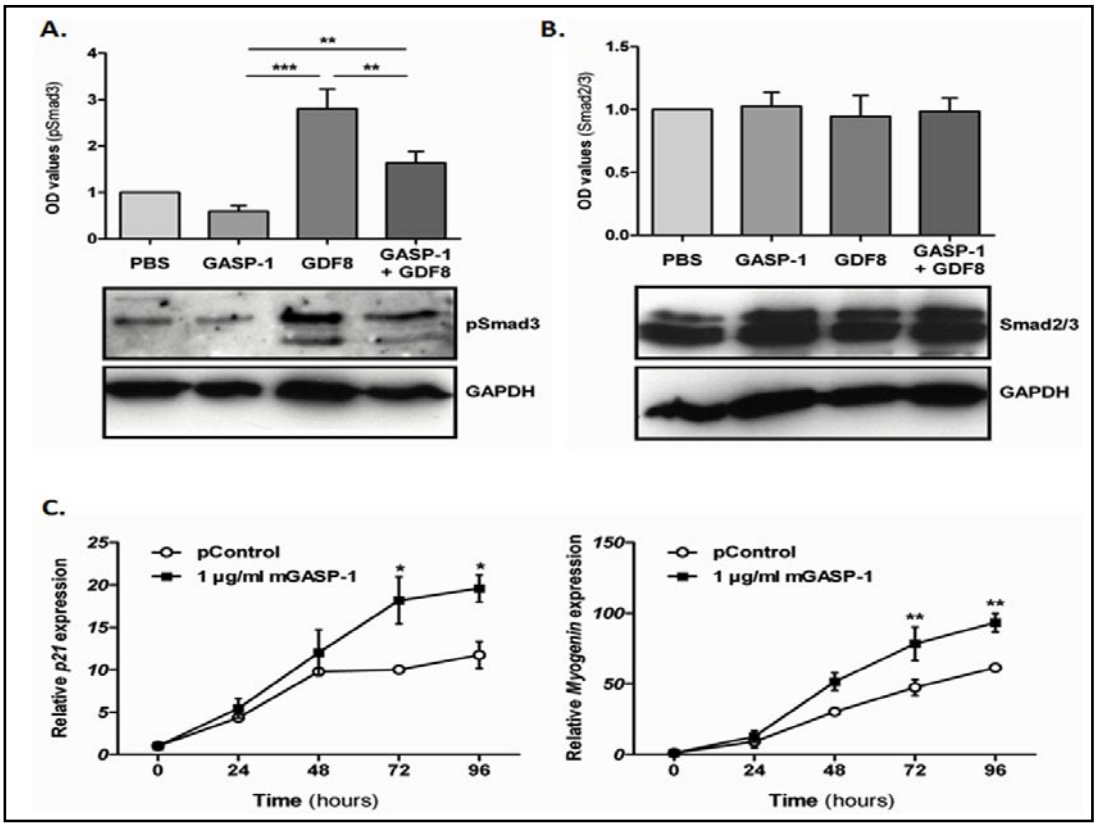

Fig. 8. Effect of mGASP-1 treatment on C2C12 myoblasts. Total proteins extracted from C2C12 treated with GDF8 (250 ng.ml^{-1}) and/or mGASP-1 (500 ng.ml^{-1}) were resolved by SDS-PAGE. (A) Membranes were immunoblotted with specific anti-pSmad3 and (B) anti-Smad2/3 antibodies. Nitrocellulose membranes were also probed with anti-GAPDH antibodies to show equal loading. The graphs were obtained using Image J software to quantify pSmad3 and Smad2/3 signals normalized with GAPDH signals of three different experiments. (C) qPCR analysis of *myogenin* and *p21* mRNA from C2C12 treated or not with 1 µg.ml^{-1} mGASP-1. Transcription levels were expressed as relative quantities compared to the initiation of differentiation (time = 0h). Each point corresponds to the mean ± S.E.M. of three experiments. Statistical significance was determined using a ANOVA analysis. A P value < 0.05 was considered significant. * : P value < 0.05; ** : P value < 0.01; *** : P value < 0.005.

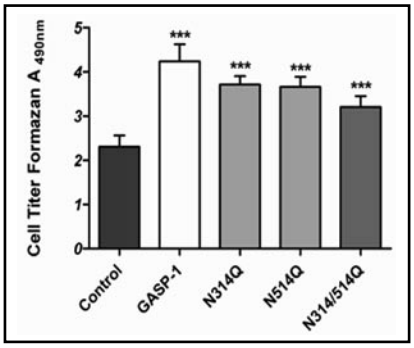

Fig. 9. Effects of mGASP-1 and *N*-glycosylation mutants on C2C12 myoblast proliferation. C2C12 myoblasts were plated at 2000 cells/well for 1 day and they grew for 48h with 1 µg.ml^{-1} of GASP-1 or its mutants, followed by Formazan assay. Data were expressed as mean ± S.D. of three different experiments. Statistical significance for all GASP-1 concentrations of 1 µg.ml^{-1} versus 0 µg.ml^{-1} was determined using ANOVA analysis. A P value < 0.05 was considered significant. *** : P value < 0.005.

However, the addition of mGASP-1 diminished the pSmad3 signal confirming that mGASP-1 inhibits the GDF8 pathway, and enhanced myogenic proliferation and differentiation (Fig. 8A). No change was shown in the Smad2/3 rates (Fig. 8B). As GDF8 decreases p21

and myogenin transcript level during C2C12 differentiation, we studied their expression and showed they were significantly up-regulated after 72h of treatment with 1 $\mu g.ml^{-1}$ of mGASP-1 compared to the untreated differentiated cells (Fig. 8C).

We also investigated whether change in site occupancy of mGASP-1 could affect its activity on myogenic proliferation by treating C2C12 myoblast cells with or without 1 $\mu g.ml^{-1}$ of each mutant protein for 48h (Fig. 9). mGASP-1, entirely glycosylated, increased the cell proliferation compared to control. Interestingly, all other *N*-glycosylation mutants acted like mGASP-1, as activators of myoblast proliferation, but with a slightly lower tendency (Fig. 9).

Discussion

In this paper, we characterized the glycosylation of secreted mGASP-1 to evaluate the effect of this post-translational modification on its bio-activity. Using bioinformatic tools, we found that the protein primary structure contains three *N*-glycosylation consensus sequences and nine potential mucin-type *O*-glycosylation sites. The latter are localized between the follistatin/Kazal and Igc2 domains, close to the region where GASP-1 interacts specifically with GDF8 [14].

We showed that the native and the recombinant mGASP-1 proteins are glycoproteins bearing both *N*- and *O*-glycans. Both type of proteins have the same migration profile on SDS-PAGE suggesting similar glycosylation states, while GASP-1 in muscular tissue of transgenic mice overexpressing GASP-1 displayed a specific four bands profile. Using different specific glycosidases, we demonstrated that this glycan macro-heterogeneity is due to the presence of *N*-linked mono- and bi-glycosylated forms of tissue-specific GASP-1. Each glycoform was found to be *O*-glycosylated or not. Our data suggested that we detected mGASP-1 over the different steps of its glycosylation in the endoplasmic reticulum and Golgi network leading to the secretion of a predominant fully glycosylated mGASP1 from skeletal muscle (Fig. 3B)

Exploring mGASP-1 function during myogenesis, we treated murine C2C12 cells with the recombinant protein. As GDF8 led to an increase of pSmad3 and a decrease of *p21* during myogenesis [19, 20], it appeared that mGASP-1 enhanced both proliferation and differentiation in a dose-dependent manner by preventing GDF8 signaling as previously reported by Bonala et al. [21].

The strong conservation of *N*-glycosylation sites among vertebrates raised our interest in investigating whether or not the *N*-glycosylation was important for mGASP-1 activity. Using site-directed mutagenesis, we produced simple, double and triple mGASP-1 mutant proteins in which asparagine of *N*-glycosylation consensus sequences were replaced by glutamine. We showed that (i) only the N314 and N514 sites are glycosylated and (ii) each mutant protein was secreted whatever its glycosylation state. Although most of the studies underline the interdependence between *N*-glycosylation and protein secretion [22], it has been reported as we, that synthesis, folding and trafficking of some glycoproteins could not be affected by altering their glycosylation status [23, 24].

We hypothesize that as GASP-1 contains several domains (WAP, follistatin/kazal, kunitz and netrin), it could have been properly, or sufficiently, folded by chaperon proteins found in the endoplasmic reticulum thus avoiding degradation. GASP-1 devoid of its *N*-glycans is *O*-glycosylated, demonstrating that the double mutant is further processed within the Golgi apparatus, secreted by the classic pathway and is not the result of a non-specific release in the culture medium by COS-7 or CHO-K1 cells. In addition, a previous work showed that bioactive GASP-1 was successfully produced and purified from a bacterial system [25]. Taken together, these data indicate that glycosylation is not necessary for some of GASP-1 functions such as anti-trypsin activity [25] and would only have a modulating role on that multifunctional protein. Nonetheless, each single mutant protein was significantly

less secreted than the native one, this is also observed for the double mutant with a more obvious effect. All the mutants were tested on C2C12 cell proliferation and surprisingly, no significant change was observed compared to the native mGASP-1, suggesting that *N*-glycans on GASP-1 do not influence its myogenic action done by modulating myostatin activity. However, their importance on other functions or circulating half-life of GASP-1 will have to be specified in the future. In particular, the presence or absence of the N514 glycan, located in the netrin domain, could be relevant in GASP-1 interaction with GDF8 propeptide or regulation of diverse serine proteases or metalloproteinases.

This study of structure-function relationships of murine GASP-1 provides for the first time more information on the involvement of the carbohydrate moiety of mGASP-1 on its inhibitor function on myostatin's actions. As GASP-1 contains multiple protein domains associated with protease-inhibitory proteins, glycan modifications may influence its other biological activities.

Acknowledgements

The authors would like to thank Dr. Benoit Laporte for his many helpful comments and suggestions. This work was supported by the French National Institute for Agricultural Research and by the Limousin Regional Council.

Conflict of Interest

The authors have declared that no competing interests exist.

References

1 Berkes CA, Tapscott SJ: MyoD and the transcriptional control of myogenesis. Semin Cell Dev Biol 2005;16:585-595.
2 Chargé SB, Rudnicki MA: Cellular and molecular regulation of muscle regeneration. Physiol Rev 2004;84:209-238.
3 Florini JR, Ewton DZ, Coolican SA: Growth Hormone and the Insulin-Like Growth Factor System in Myogenesis. Endocr Rev 1996;17:481-517.
4 Li L, Zhou J, James G, Heller-Harrison R, Czech MP, Olson EN: FGF inactivates myogenic helix-loop-helix proteins through phosphorylation of a conserved protein kinase C site in their DNA-binding domains. Cell 1992;71:1181-1194.
5 Liu D, Black BL, Derynck R: TGF-β inhibits muscle differentiation through functional repression of myogenic transcription factors by Smad3. Gene Dev 2001;15:2950–2966.
6 Lynch GS, Schertzer JD, Ryall JG: Therapeutic approaches for muscle wasting disorders. Pharmacol Ther 2007;113:461-487.
7 Carnac G, Vernus B, Bonnieu A: Myostatin in the pathophysiology of skeletal muscle. Curr Genomics 2007;8:415-422.
8 Lee SJ: Regulation of muscle mass by myostatin. Annu Rev Cell Dev Biol 2004;20:61-86.
9 McPherron AC, Lawler AM, Lee SJ: Regulation of skeletal muscle mass in mice by a new TGF-beta superfamily member. Nature 1997;387:83-90.
10 Haidet AM, Rizo L, Handy C, Umapathi P, Eagle A, Shilling C: Long-term enhancement of skeletal muscle mass and strength by single gene administration of myostatin inhibitors. Proc Natl Acad Sci USA 2008;105:4318-4322.

11 Lee SJ, McPherron AC: Regulation of myostatin activity and muscle growth. Proc Natl Acad Sci USA 2001;98:9306-9311.
12 Hill JJ, Qiu Y, Hewick RM, Wolfman NM: Regulation of myostatin in vivo by growth and differentiation factor-associated serum protein-1: a novel protein with protease inhibitor and follistatin domains. Mol Endocrinol 2003;17:1144-1154.
13 Szláma G, Kondás K, Trexler M, Patthy L: WFIKKN1 and WFIKKN2 bind growth factors TGFβ1, BMP2 and BMP4 but do not inhibit their signalling activity. FEBS J 2010;277:5040-5050.
14 Kondás K, Szláma G, Trexler M, Patthy L: Both WFIKKN1 and WFIKKN2 have high affinity for growth and differentiation factors 8 and 11. J Biol Chem 2008;283:23677-23684.
15 Varki A, Lowe JB: Biological Roles of Glycans; in: Varki A, Cummings RD, Esko JD, Freeze HH, Stanley P, Bertozzi CR, Hart GW, Etzler ME (eds): Source Essentials of Glycobiology. 2nd edition. Cold Spring Harbor, NY, Cold Spring Harbor Laboratory Press, 2009, Chapter 6.
16 Cummings RD: 2005. Glycosylation. Encyclopedia of Genetics, Genomics, Proteomics and Bioinformatics. DOI: 10.1002/047001153X.g305106. John Wiley & Sons, Ltd.
17 Julenius K, Mølgaard A, Gupta R, Brunak S: Prediction, conservation analysis, and structural characterization of mammalian mucin-type *O*-glycosylation sites. Glycobiology 2005;15:153-164.
18 Saremi A, Gharakhanloo R, Sharghi S, Gharaati MR, Larijani B, Omidfar K: Effects of oral creatine and resistance training on serum myostatin and GASP-1. Mol Cell Endocrinol 2010;317:25-30.
19 Thomas M, Langley B, Berry C, Sharma M, Kirk S, Bass J, Kambadur R: Myostatin, a negative regulator of muscle growth, functions by inhibiting myoblast proliferation. J Biol Chem 2000;275:40235-40243.
20 Langley B, Thomas M, Bishop A, Sharma M, Gilmour S, Kambadur R: Myostatin inhibits myoblast differentiation by down-regulating MyoD expression. J Biol Chem 2002;277:49831-49840.
21 Bonala S, Lokireddy S, Arigela H, Teng S, Wahli W, Sharma M, McFarlane C, Kambadur R: Peroxisome Proliferator-activated Receptor β/δ Induces Myogenesis by Modulating Myostatin Activity. J Biol Chem 2012;287:12935-12951.
22 Roth J, Zuber C, Park S, Jang I, Lee Y, Kysela KG, Le Fourn V, Santimaria R, Guhl B, Cho JW: Protein N-glycosylation, protein folding, and protein quality control. Mol Cells 2010;30:497-506.
23 Kruszewska JS, Perlińska-Lenart U, Górka-Niec W, Orlowski J, Zembek P, Palamarczyk G: Alterations in protein secretion caused by metabolic engineering of glycosylation pathways in fungi. Acta Biochemica Polona 2008;3:447-456.
24 Takashima S, Amano J: Glycosylation and secretion of human α-amylases. Advances in Biological Chemistry 2012;2:10-19.
25 Kondás K, Szláma G, Nagy A, Trexler M, Patthy L: Biological functions of the WAP domain-containing multidomain proteins WFIKKN1 and WFIKKN2. Biochem Soc Trans 2011;39:1416-1420.